

This discussion paper is/has been under review for the journal Hydrology and Earth System Sciences (HESS). Please refer to the corresponding final paper in HESS if available.

# Assessment of the indirect calibration of a rainfall-runoff model for ungauged catchments in Flanders

N. De Vleeschouwer<sup>1</sup> and V. R. N. Pauwels<sup>2</sup>

<sup>1</sup>Laboratory of Hydrology and Water Management, Ghent University, Ghent, Belgium

<sup>2</sup>Department of Civil Engineering, Monash University, Clayton, Victoria, Australia

Received: 29 November 2012 – Accepted: 11 December 2012 – Published: 7 January 2013

Correspondence to: N. De Vleeschouwer (niels.devleeschouwer@ugent.be)

Published by Copernicus Publications on behalf of the European Geosciences Union.

**HESSD**

10, 103–144, 2013

## Assessment of indirect calibration

N. De Vleeschouwer and  
V. R. N. Pauwels

Title Page

Abstract

Introduction

Conclusions

References

Tables

Figures

◀

▶

◀

▶

Back

Close

Full Screen / Esc

Printer-friendly Version

Interactive Discussion



## Abstract

In this paper the potential of discharge-based indirect calibration of the Probability Distributed Model (PDM), a lumped rainfall-runoff (RR) model, is examined for six selected catchments in Flanders. The concept of indirect calibration indicates that one has to estimate the calibration data because the catchment is ungauged. A first case in which indirect calibration is applied is that of spatial gauging divergence: Because no observed discharge records are available at the outlet of the ungauged catchment, the calibration is carried out based on a rescaled discharge time series of a very similar donor catchment. Both a calibration in the time domain and the frequency domain (a.k.a. spectral domain) are carried out. Furthermore, the case of temporal gauging divergence is considered: Limited (e.g. historical or very recent) discharge records are available at the outlet of the ungauged catchment. Additionally, no time overlap exists between the forcing and discharge records. Therefore, only an indirect spectral calibration can be performed in this case. To conclude also the combination case of spatio-temporal gauging divergence is considered. In this last case only limited discharge records are available at the outlet of a donor catchment. Again the forcing and discharge records are not contemporaneous which only makes feasible an indirect spectral calibration. The modelled discharge time series are found to be acceptable in all three considered cases. In the case of spatial gauging divergence, indirect temporal calibration results in a slightly better model performance than indirect spectral calibration. Furthermore, indirect spectral calibration in the case of temporal gauging divergence leads to a better model performance than indirect spectral calibration in the case of spatial gauging divergence. Finally, the combination of spatial and temporal gauging divergence does not necessarily lead to a worse model performance compared to the separate cases of spatial and temporal gauging divergence.

## Assessment of indirect calibration

N. De Vleeschouwer and  
V. R. N. Pauwels

Title Page

Abstract

Introduction

Conclusions

References

Tables

Figures



Back

Close

Full Screen / Esc

Printer-friendly Version

Interactive Discussion



# 1 Introduction

The practical application of RR models requires a proper assignment of the parameter values, also known as the process of parametrisation or calibration (Duan et al., 1992). Ideally, this calibration process should be fed by in situ measurements or remote sensing data. Practical considerations, however, implicate an alternative strategy. In a classic calibration framework the parameter values are adjusted until the match between the modelled and observed output (e.g. discharge) is found to be acceptable. As hydrologic models increasingly become more sophisticated, the iterative parameter adjustments are usually performed by specific optimisation algorithms. Commonly used algorithms in hydrologic modelling are e.g. genetic algorithms (Reed et al., 2000) like the Shuffled Complex Evolution Algorithm (SCE-UA) (Duan et al., 1992), local and multistart simplex methods (Gan and Biftu, 1996), Particle Swarm Optimisation (PSO) (Kennedy and Eberhart, 1995; Scheerlinck et al., 2009), Simulated Annealing (SA) (Thyer et al., 1999), etc. In practice the conditions to perform an ordinary direct calibration are not always fulfilled. This implies an indirect calibration strategy. In the past decade, the research concerning indirect calibration has gained attention in the hydrologic community through the Prediction in Ungauged Basins (PUB) initiative (Sivapalan et al., 2003) set up by the International Association of Hydrological Sciences (IAHS). In scarcely gauged regions, discharge records may lack entirely for the catchment of interest, and may only be available at the outlet of a nearby catchment. This situation will be indicated in this paper by the term “spatial gauging divergence”. In many catchments forcings (e.g. precipitation) and discharges have not been recorded contemporaneously. Consequently, the modelled discharge cannot be compared to the observations. Hereafter, this case will be indicated by the term “temporal gauging divergence”. In case of an indirect calibration approach it can be expected that the resulting predictive power of the model will be lower than the predictive power obtained by an ordinary direct calibration. Therefore, the research question is whether an acceptable predictive power of the model can be obtained in a certain case of gauging divergence.

## Assessment of indirect calibration

N. De Vleeschouwer and  
V. R. N. Pauwels

Title Page

Abstract

Introduction

Conclusions

References

Tables

Figures



Back

Close

Full Screen / Esc

Printer-friendly Version

Interactive Discussion



**Assessment of  
indirect calibration**N. De Vleeschouwer and  
V. R. N. Pauwels

Title Page

Abstract

Introduction

Conclusions

References

Tables

Figures

◀

▶

◀

▶

Back

Close

Full Screen / Esc

Printer-friendly Version

Interactive Discussion



One of the techniques useful for parameter estimation in ungauged catchments is spectral calibration (Montanari and Toth, 2007; Winsemius et al., 2009; Quets et al., 2010; Pauwels and De Lannoy, 2011). In the ordinary form the spectral properties (e.g. the spectral density  $S$ ) of both the observed and modelled output are matched instead of the time series themselves. In order to obtain those properties one has to perform a transformation of the time series to the frequency domain. In the aforementioned cases of spatial and temporal gauging divergence it is impossible to carry out a direct spectral calibration because observed outputs are missing in the calibration period for the catchment under consideration. Consequently the spectral properties of the non observed discharge response need to be estimated. Montanari and Toth (2007) first illustrated the opportunities of indirect spectral calibration in hydrological modelling using a maximum likelihood estimator proposed by Whittle (1953). Under the condition of periodicity, the spectral densities of two observed time series separated in time have a higher degree of agreement than the observations in the time domain. This demonstrates the possibility of obtaining a proper estimate of the spectral density of a time series based on non-contemporaneous records. Furthermore, it is possible to carry out the calibration in absence of discharge records at the outlet of the considered catchment. The spectral density estimates can then be based on discharge time series in nearby catchments.

In this paper indirect calibration is applied to the PDM (Moore, 2007) for six catchments in Flanders. By alternately considering these catchments gauged and ungauged, indirect calibration can be compared to direct calibration in terms of the predictive power of the RR model. Both the cases of spatial and temporal gauging divergence are examined. Additionally, the combination of temporal and spatial gauging divergence is considered.

## 2 Spectral properties: mathematical background

The spectral densities  $S$  of a time series without missing records can be approximated by calculating the periodogram  $c^2$  which requires a transformation of the time series to the frequency domain. The discharge time series  $Q(t)$  consisting of  $D$  equally long time steps ( $t \in [1, \dots, D]$ ) can be written as a Fourier series:

$$Q(t) = \sum_{k=0}^N \Psi(k) \left[ a(k) \cos\left(\frac{2\pi k}{D}(t-1)\right) + b(k) \sin\left(\frac{2\pi k}{D}(t-1)\right) \right]. \quad (1)$$

$k \in [0, \dots, N]$  is the harmonic number. This variable determines the wavelength  $\lambda$  of the terms through the relationship  $\lambda = \frac{L}{k}$ ,  $L$  being the length of the time series. The spectral densities in function of the harmonic number are also called the density spectrum. If the time series consists of an even number of time steps, the highest harmonic  $N = \frac{D}{2}$  (Shannon, 1984) and  $\Psi(k) \in [\frac{1}{2}, 1, \dots, 1, \frac{1}{2}]$ . If this is not the case, then  $N = \frac{D-1}{2}$  and  $\Psi(k) \in [\frac{1}{2}, 1, \dots, 1]$ .  $a(k)$  and  $b(k)$  are referred to as Fourier coefficients. The periodogram is calculated as  $c^2(k) = \Psi(k^2)(a^2(k) + b^2(k))$ .

Since discharge time series usually contain record gaps it is often not possible to perform this computationally efficient approximation of the discharge density spectrum. Therefore, the latter has to be calculated directly through the Wiener–Khinchine relationship (Papoulis, 1965; Brown and Hwang, 1992):

$$S(k) = \mathcal{F}[R(\tau)]. \quad (2)$$

$\mathcal{F}$  stands for the Fourier transformation.  $R(\tau)$ , known as the correlation function in signal processing disciplines, is calculated as follows:

$$R(\tau) = E[Q(t)Q(t-\tau)]. \quad (3)$$

Herein  $\tau$  stands for the temporal lag. For the calculation periodicity of the time series is assumed. Calculating the entire correlation function ( $\tau \in [0, 1, \dots, D-1]$ ) becomes computationally intensive in case of long time series. For this reason lower values are chosen for the maximum lag  $\tau_{\max}$  in this paper. Consequently, the resulting variables are

## Assessment of indirect calibration

N. De Vleeschouwer and  
V. R. N. Pauwels

Title Page

Abstract

Introduction

Conclusions

References

Tables

Figures

◀

▶

◀

▶

Back

Close

Full Screen / Esc

Printer-friendly Version

Interactive Discussion



only approximations of the spectral density  $S$ . However, for simplicity, these variables will yet be referred to as spectral densities in the remainder of this paper.

### 3 Model description

In this study the PDM, a lumped RR model, is used to simulate the discharge response in the considered catchments. The model basically consists of three storages to represent the water flowpaths (see Fig. 1). The probabilistic distributed soil moisture storage  $S_1$  [mm] receives the net precipitation input ( $P - aET$ ) [mm],  $P$  [mm] and  $aET$  [mm], respectively being the gross precipitation and actual evapotranspiration. Based on the concept of Dunnian runoff (Dunne and Black, 1970) the net precipitation is partitioned into direct runoff  $Q_{di}$  [mm] and drainage  $Q_{dr}$  [mm]. The former is converted to surface runoff  $Q_r$  [mm] through a fast surface storage (cascade of two linear reservoirs), the latter to base flow  $Q_b$  [mm] through a slow subsurface storage. The sum of surface runoff and base flow equals the total discharge  $Q_t$  [mm]. The more detailed mathematical description of the PDM can be found in Appendix A. The model version in this research makes use of 12 parameters. An overview is given in Table 1. Additionally, the estimated lower and upper boundaries of these parameters in Flemish catchments are provided (Cabus, 2008).

### 4 Site description and data availability

Figure 2 shows a preselection of 32 catchments in the Scheldt and Yser basins in Flanders. The drainage areas range from 2 to 265 km<sup>2</sup>. The size of the catchments considered in this study is thus rather small. The catchments are delineated based on a Digital Elevation Model (DEM) with a spatial resolution of 25 m using the algorithms described in Jenson and Domingue (1988). For every catchment hourly discharge records are available at the outlet for five consecutive years (2006–2010). Hourly precipitation and

## Assessment of indirect calibration

N. De Vleeschouwer and  
V. R. N. Pauwels

Title Page

Abstract

Introduction

Conclusions

References

Tables

Figures

◀

▶

◀

▶

Back

Close

Full Screen / Esc

Printer-friendly Version

Interactive Discussion



potential evapotranspiration forcing records were obtained from the Flemish Environment Agency (VMM) monitoring network. Precipitation and potential evapotranspiration time series were available for the period 2005–2010 in, respectively 14 and 4 meteo stations (see Fig. 2). The year 2005 is used to initialise the PDM. Catchment specific forcing data were obtained using inverse square distance weighing (see Eq. 4). It was decided to only include the three most nearby meteo stations in the interpolation ( $N = 3$ ).

$$z(x_i, y_i, t) = \sum_{k=1}^N \frac{\left[ (x_i - x_k)^2 + (y_i - y_k)^2 \right]^{-1}}{\sum_{j=1}^N \left[ (x_i - x_j)^2 + (y_i - y_j)^2 \right]^{-1}} z(x_k, y_k, t) \quad (4)$$

Herein  $z(x_i, y_i, t)$  is the interpolated forcing  $z$  at the point of gravity  $(x_i, y_i)$  of catchment  $i$  at timestep  $t$ .  $z(x_k, y_k, t)$  is the forcing record measured at the  $k$ -th meteo station out of  $N$  at location  $(x_k, y_k)$  and at timestep  $t$ . Furthermore, raster data with a spatial resolution of 25m regarding land cover and soil type were obtained from the Flemish Geographical Information Agency (FGIA).

A subgroup of six catchments (see Table 2) is further selected for the calibration experiments. In the remainder of this paper these catchments are considered to be ungauged and will be referred to with the term “autochtone catchments”. The subgroup is chosen in order to obtain a certain diversity with respect to geographical location, drainage area, land cover, soil type, geomorphology and morphometry. In this way a certain bias in the conclusions of the calibration experiments should be minimised. In Fig. 2 the autochtone catchments are colored gray.

## Assessment of indirect calibration

N. De Vleeschouwer and  
V. R. N. Pauwels

Title Page

Abstract

Introduction

Conclusions

References

Tables

Figures

⏪

⏩

◀

▶

Back

Close

Full Screen / Esc

Printer-friendly Version

Interactive Discussion



## 5 Estimation of the spectral densities

### 5.1 Case of spatial gauging divergence

In order to estimate the density spectrum of the autochtone discharge time series in the case of spatial gauging divergence, a donor catchment approach is introduced. This implies for every autochtone catchment the identification of the catchment in the population of 31 remaining catchments with the most similar discharge density spectrum. In practice, this identification has to be performed indirectly because the autochtone density spectrum is unknown. In this research a selection based on five catchment properties is proposed to identify the best donor catchment. The difference in drainage area and the mutual distance between the points of gravity are considered to be the most determining properties. The drainage area is an important indicator of the discharge magnitude and thus the spectral density magnitude. The drainage area dissimilarity between catchments  $i$  and  $j$  is expressed by a normalised dissimilarity index  $NDI_A$ :

$$NDI_A(i, j) = \frac{|A_i - A_j|}{A_{\max} - A_{\min}}. \quad (5)$$

$A_i$  is the drainage area of catchment  $i$ . The subscripts max and min indicate, respectively the highest and lowest drainage area value in the population of 32 catchments. The mutual distance between the points of gravity of two catchments can serve as a measure for the difference in the observed meteorologic pattern. Significant differences in the latter can be reflected in the spectral properties of the discharge time series. The normalised dissimilarity with respect to the mutual distance is calculated by the  $NDI_D$ :

$$NDI_D(i, j) = \frac{D_{i,j}}{D_{\max}}. \quad (6)$$

$D_{i,j}$  is the distance between catchment  $i$  and  $j$ .  $D_{\max}$  is the maximum distance between two catchments in the population. Another catchment property having an influence on

## Assessment of indirect calibration

N. De Vleeschouwer and  
V. R. N. Pauwels

Title Page

Abstract

Introduction

Conclusions

References

Tables

Figures



Back

Close

Full Screen / Esc

Printer-friendly Version

Interactive Discussion



the spectral density of a discharge time series is the land topography. For instance, steeper catchments are generally characterised by a higher surface runoff. Therefore, the high frequency parts of the discharge density spectrum (large  $k$ ) will be higher than will be the case in horizontal catchments. In order to let this property interfere in the selection of the donor catchments the following normalised dissimilarity index is introduced:

$$\text{NDI}_R(i, j) = \frac{|S_{me,i} - S_{me,j}|}{S_{me,max} - S_{me,min}}. \quad (7)$$

$S_{me,i}$  is the mean local slope of catchment  $i$ . The local slope is calculated at the grid cell scale. The subscripts max and min indicate, respectively the highest and lowest mean local slope in the population of 32 catchments. Soil composition and land cover are also incorporated in the selection framework. Both properties have an important influence on the infiltration rate and thus the runoff in a catchment. Therefore, soil composition and land cover can possibly have a proper influence on the pattern of the discharge density spectrum. The  $\text{NDI}_S$  and  $\text{NDI}_L$  are proposed to, respectively account for dissimilarities in soil composition and land cover.

$$\text{NDI}_S(i, j) = \sum_{k=1}^{N_B} \phi_k \frac{|\text{sc}\%_{k,i} - \text{sc}\%_{k,j}|}{\text{sc}\%_{k,max} - \text{sc}\%_{k,min}} \quad (8)$$

$$\text{NDI}_L(i, j) = \sum_{k=1}^{N_L} \chi_k \frac{|\text{lc}\%_{k,i} - \text{lc}\%_{k,j}|}{\text{lc}\%_{k,max} - \text{lc}\%_{k,min}}. \quad (9)$$

$N_B$  and  $N_L$  are the number of soil and land cover classes. The relative areas of a certain soil or landcover class  $k$  are presented by  $\text{sc}\%_k$  and  $\text{lc}\%_k$ . Again, the highest and lowest values for the considered variables are indicated with, respectively the subscripts max and min. Important to notice are the weights  $\phi_k$  and  $\chi_k$ . Those are equal to the mean relative area of a particular soil or land cover class in the two catchments to be

## Assessment of indirect calibration

N. De Vleeschouwer and  
V. R. N. Pauwels

Title Page

Abstract

Introduction

Conclusions

References

Tables

Figures

◀

▶

◀

▶

Back

Close

Full Screen / Esc

Printer-friendly Version

Interactive Discussion



compared. In this way rare soil or land cover classes cannot have a large influence on the donor catchment selection.

To assess the total dissimilarity between two catchments a weighted sum of the aforementioned indices is calculated. In this study the following weights are used: 0.3 for the  $NDI_A$  and  $NDI_D$ , 0.2 for the  $NDI_S$  and 0.1 for the  $NDI_B$  and  $NDI_L$ . For every autochtone catchment the catchment with the lowest general dissimilarity is selected as the donor catchment. Table 3 gives an overview of the selected donor catchments. The same order is preserved as in Table 2, so for example catchment Reninge–Kemmelbeek is the donor catchment for catchment Merkem–Martjevaart. In Fig. 2 the six donor catchments are filled in with a diagonal line pattern.

Subsequently, a rescaling of the donor discharge records is performed in order to improve the autochtone time series estimate. This rescaling (see Eq. 10) is based on the drainage area of the autochtone and donor catchment because of the proper linear relationship (Pearson correlation coefficient  $R = 0.87$ ) between mean discharge (period 2006–2009) and the drainage area in the population of 32 Flemisch catchments.

$$\hat{Q}_{\text{aut}}(t) = \frac{A_{\text{aut}}}{A_{\text{don}}} Q_{\text{don}}(t). \quad (10)$$

$\hat{Q}_{\text{aut}}(t) [\text{m}^3 \text{s}^{-1}]$  is the estimated autochtone discharge time series,  $Q_{\text{don}}(t) [\text{m}^3 \text{s}^{-1}]$  is the donor discharge time series.  $A_{\text{aut}} [\text{km}^2]$  and  $A_{\text{don}} [\text{km}^2]$  are the drainage areas of, respectively the autochtone and donor catchment. Based on the aforementioned relationship between a time series and the corresponding spectral density spectrum, the estimated density spectrum of the autochtone catchment  $\hat{S}_{\text{aut}}(k) [\text{m}^6 \text{s}^{-2}]$  can be calculated as follows:

$$\hat{S}_{\text{aut}}(k) = \frac{A_{\text{aut}}^2}{A_{\text{don}}^2} S_{\text{don}}(k). \quad (11)$$

Herein  $S_{\text{don}}(k) [\text{m}^6 \text{s}^{-2}]$  is the density spectrum of the donor discharge records. In Figs. 3 ( $k = 0$ ) and 4 ( $k > 0$ ) the actual and estimated root squared spectral densities

## Assessment of indirect calibration

N. De Vleeschouwer and  
V. R. N. Pauwels

Title Page

Abstract

Introduction

Conclusions

References

Tables

Figures

◀

▶

◀

▶

Back

Close

Full Screen / Esc

Printer-friendly Version

Interactive Discussion



of the discharge time series (period 2006–2009) in the six autochtone catchments are presented. The maximum time lag  $\tau_{\max}$  considered is 3 months. For certain catchments (e.g. Oostkamp–Rivierbeek and Bertem–Voer) a good match is obtained. This is however not the case for all catchments (e.g. Merkem–Martjevaart: spectral density for  $k = 0$ , Rummen–Melsterbeek: spectral densities for  $k > 0$ ).

## 5.2 Case of temporal gauging divergence

The assumption of periodicity has as consequence an invariable density spectrum. In the case of temporal gauging divergence it is thus assumed that the density spectrum of the limited non overlapping discharge time series is a good estimate of the density spectrum of the time series overlapping with the forcing records. In Fig. 5 ( $k = 0$ ) and 6 ( $k > 0$ ) the root squared density spectrums of the periods 2006–2007 and 2008–2009 are compared for the six catchments under consideration. A proper match is found, and this to a greater extent for the high frequency parts of the spectrums.

## 6 Calibration and validation

### 6.1 Test setup

In this section, different calibration experiments are carried out in order to optimise the PDM for the autochtone catchments considered in this study. The calibration period runs from 1 January 2006 through 31 December 2009. 2005 serves as a initialisation year for the RR model. The first experiment encompasses a comparison between direct temporal calibration and direct spectral calibration. With regard to the latter, also the relationship between the maximum lag  $\tau_{\max}$  of the correlation function and the resulting model performance is examined. Furthermore the effect of assigning more weight to particular parts of the density spectrum in the objective function is examined. In a second experiment, the case of spatial gauging divergence is further examined. Direct spectral calibration is compared to indirect calibration in the time and frequency

## Assessment of indirect calibration

N. De Vleeschouwer and  
V. R. N. Pauwels

Title Page

Abstract

Introduction

Conclusions

References

Tables

Figures

◀

▶

◀

▶

Back

Close

Full Screen / Esc

Printer-friendly Version

Interactive Discussion



domain. For both indirect calibration setups the estimates for, respectively the time series and spectral density are based on discharge records at the outlet of the donor catchments. The third experiment focusses on the case of temporal gauging divergence. The autochtone discharge time series used in the calibration is limited and does not overlap with the forcing records. Additionally, in a fourth experiment a non overlapping donor discharge time series is used in the calibration to examine the combined effect of spatial and temporal gauging divergence on the calibration of the hydrological model. The code names and properties of all calibration setups are listed in Table 4.

Each calibration setup is applied three times for every autochtone catchment. All repeated optimisations are assessed using four indicators: the Pearson correlation coefficient ( $R$ ), the relative absolute bias (BIASn), the relative Root Mean Square Error (RMSEn) and the Nash-Sutcliffe coefficient (NS):

$$R = \frac{\sum_{t=1}^n [Q_{\text{obs}}(t) - \bar{Q}_{\text{obs}}][Q_{\text{sim}}(t) - \bar{Q}_{\text{sim}}]}{\sqrt{\sum_{t=1}^n [Q_{\text{obs}}(t) - \bar{Q}_{\text{obs}}]^2} \sqrt{\sum_{t=1}^n [Q_{\text{sim}}(t) - \bar{Q}_{\text{sim}}]^2}} \quad (12)$$

$$\text{BIASn} = \frac{1}{\bar{Q}_{\text{obs}}} \left| \frac{1}{n} \sum_{t=1}^n [Q_{\text{obs}}(t) - Q_{\text{sim}}(t)] \right| \quad (13)$$

$$\text{RMSEn} = \frac{1}{\bar{Q}_{\text{obs}}} \sqrt{\frac{1}{n} \sum_{t=1}^n [Q_{\text{obs}}(t) - Q_{\text{sim}}(t)]^2} \quad (14)$$

$$\text{NS} = 1 - \frac{\sum_{t=1}^n [Q_{\text{obs}}(t) - Q_{\text{sim}}(t)]^2}{\sum_{t=1}^n [Q_{\text{obs}}(t) - \bar{Q}_{\text{obs}}]^2} \quad (15)$$

**Assessment of indirect calibration**

N. De Vleeschouwer and  
V. R. N. Pauwels

Title Page

Abstract

Introduction

Conclusions

References

Tables

Figures

◀

▶

◀

▶

Back

Close

Full Screen / Esc

Printer-friendly Version

Interactive Discussion



## Assessment of indirect calibration

N. De Vleeschouwer and  
V. R. N. Pauwels

Title Page

Abstract

Introduction

Conclusions

References

Tables

Figures

◀

▶

◀

▶

Back

Close

Full Screen / Esc

Printer-friendly Version

Interactive Discussion



$Q_{\text{obs}} [\text{m}^3 \text{s}^{-1}]$  and  $Q_{\text{sim}} [\text{m}^3 \text{s}^{-1}]$  are, respectively the observed and simulated discharge values.  $\bar{Q}_{\text{obs}}$  and  $\bar{Q}_{\text{sim}}$  are, respectively the mean observed and simulated discharge. For every autochtone catchment and calibration setup the assessment indicators of the repetition characterised by the lowest RMSEn are retained. The absolute bias and RMSE are divided by the mean observed discharge in order to obtain four dimensionless indicators. In this form it is possible to average the retained indicators over the six catchments without giving more weight to the indicators of catchments characterised by a high mean discharge.

The calibration algorithm applied in this research is Particle Swarm Optimisation (PSO) (Kennedy and Eberhart, 1995). The ability of PSO to find optimal solutions for hydrological modelling issues has already been demonstrated in various studies (Gill et al., 2006; Scheerlinck et al., 2009; Tolson et al., 2009; Zhang and Chiew, 2009; Mousavi and Shourian, 2010; Liu and Han, 2010; Pauwels and De Lannoy, 2011). This swarm intelligence algorithm is based on the movement of different particles throughout the  $n$ -dimensional parameter space. This movement is controlled by the particle's own history of positions (and thus related values of the objective function) and that of neighbouring particles, resulting in a so-called global behaviour. In order to adjust this behaviour so that a convergence to the global optimum is found, a parametrisation of the calibration algorithm is required. The type of PSO applied in this paper is characterised by the parameter vector  $\psi = [N_i N_k c_1 c_2 w \delta]^T$  (description parameters see Table 5).

$N_i$  and  $N_k$  are assigned a value of, respectively 30 and 36 (Pauwels and De Lannoy, 2011). The values of the remaining parameters are selected out of the following discrete intervals, also applied in Pauwels and De Lannoy (2011):

1.  $c_1 \in \{0.8, 1.0, \dots, 1.8\}$
2.  $c_2 \in \{1.0, 1.2, \dots, 2.2\}$
3.  $w \in \{0.2, 0.4, 0.6\}$

4.  $\delta \in \{0.2, 0.4, 0.6\}$ .

For every parameter combination a direct temporal calibration of the PDM is performed for the catchment Merkem–Martjevaart. The selection of the optimal parameter vector is based on the RMSE between the  $n$  observed discharge records  $Q_{\text{obs}}$  and model simulations  $Q_{\text{sim}}$ . The lowest RMSE ( $0.637 \text{ m}^3 \text{ s}^{-1}$ ) is found with  $\psi = [30361.82.20.20.4]^T$ . There is a problem of equifinality (Beven and Binley, 1992) as a high amount of parameter combinations give near optimal RMSE's. Due to practical considerations the above mentioned most optimal set is applied in all of the following calibration setups.

The model calibration is followed by a validation. The validation period runs from 1 January 2010 till 31 December 2010. For this the year 2009 is used to initialise the PDM. As in the calibration the same four dimensionless indicators are used (averaged over the six autochtone catchments) to make an assessment of the calibration setups.

## 6.2 Results and discussion

### 6.2.1 Experiment 1: direct temporal vs. spectral calibration

In this first experiment direct temporal calibration is compared to direct spectral calibration. With regard to the former the RMSE between the observed and simulated discharges is used as objective function. Spectral calibration on the other hand makes use of of a spectral objective function. For example this can be the RMSE between the spectral densities of the observed and simulated time series. However, better results are achieved by an RMSE between the root squared spectral densities (Quets et al., 2010; Pauwels and De Lannoy, 2011). The latter is thus applied in this research. First, the influence of the maximum lag of the correlation function  $\tau_{\text{max}}$  on the post calibration model performance is examined. Three values for  $\tau_{\text{max}}$  are proposed: 1, 3 and 12 months. In Fig. 7 (upper-left subplot) the averaged assessment indicators for the calibration period (2006–2009) are compared for setups T-D, F-D-1-0, F-D-3-0 and F-D-12-0. It is clear that discharge is mostly better simulated after a calibration in the

## Assessment of indirect calibration

N. De Vleeschouwer and  
V. R. N. Pauwels

Title Page

Abstract

Introduction

Conclusions

References

Tables

Figures

◀

▶

◀

▶

Back

Close

Full Screen / Esc

Printer-friendly Version

Interactive Discussion



time domain (higher  $R$  and NS coefficient, lower BIASn and RMSEn). A clearly poorer model performance can be noted when applying a low  $\tau_{\max}$ . This is probably due to the information loss which is a consequence of the limitation of the correlation function. As can be expected in the validation period (see Fig. 7, upper-right subplot) the BIASn and RMSEn are remarkably higher for all four setups compared to the calibration period. This is however not the case for the  $R$  and NS coefficient. Furthermore, the setups relate differently with regard to model performance. For three out of four assessment indicators temporal calibration still leads to better results, however the differences with spectral calibration using a  $\tau_{\max}$  of 3 months are very small. With respect to the relative RMSEn even better simulations are obtained after calibration in the frequency domain if  $\tau_{\max}$  is 1 or 3 months. Spectral calibration with the longest correlation function ( $\tau_{\max} = 12$  months) leads to a remarkably higher BIASn and RMSEn and to a lesser extent also to a lower  $R$  and NS coefficient. This may be due to an overfitting of the data. Because of this observation a  $\tau_{\max}$  value of 3 months is proposed for all following spectral calibration setups. A second influence on the calibration exercise examined in this experiment is giving weights to certain parts of the density spectrum in the objective function. This is performed by the principle of exponential clustering (see Fig. 8). Three types of weights are proposed:

- Type 1: the spectral densities for  $k < 9$  retain their value. Exponential clustering and averaging over those clusters is applied from  $k = 9$  to  $k = N$ . Higher weights are thus assigned to the low frequency part of the density spectrum.
- Type 2: the spectral density for  $k = 0$  is not considered in the objective function. Exponential clustering and averaging over those clusters is applied from  $k = 1$  to  $k = N$ . Higher weights are thus assigned to the low frequency part of the density spectrum with a zero weight for the first spectral density.
- Type 3: exponential clustering and averaging over those clusters is applied from  $k = N$  to  $k = 0$ . Higher weights are thus assigned to the high frequency part of the density spectrum.

**Assessment of indirect calibration**N. De Vleeschouwer and  
V. R. N. Pauwels

Title Page

Abstract

Introduction

Conclusions

References

Tables

Figures

◀

▶

◀

▶

Back

Close

Full Screen / Esc

Printer-friendly Version

Interactive Discussion



It can be concluded from Fig. 7 (middle subplots) that giving weights to certain parts of the density spectrum generally does not lead to a better model performance in the calibration and validation period. This applies to a greater extent for weight type 3 or thus to giving more weight to the high frequency part of the density spectrum. It is also clear that not taking into account the density for  $k = 0$  leads to a high BIASn. This can be explained by the relationship between the spectral density at  $k = 0$  and the mean of a time series. If  $\tau_{\max} = D - 1$ , then this first density equals the squared mean of the time series. Not taking into account the first spectral density thus results in no explicit matching of the means of the observed and simulated time series. Because of the aforementioned conclusions no types of weight are applied in the indirect spectral calibrations of experiment 2, 3 and 4.

### 6.2.2 Experiment 2: indirect spectral calibration in case of spatial gauging divergence (setup F-IS-3-0)

This second calibration experiment focusses on the discharge prediction in an autochtone catchment without available discharge records at the outlet. However, discharge records are available at the outlet of a donor catchment in the same time window as the forcing records monitored in the autochtone catchment (spatial gauging divergence). Two calibration strategies are undertaken: a temporal calibration on the rescaled donor discharges (see Eq. 10) (setup T-IS) and a spectral calibration on the root squared spectral densities of the rescaled donor discharges (see Eq. 11) (setup F-IS-3-0). A first observation in the calibration period (see Fig. 7, lower-left subplot) is the reduced model performance after an indirect calibration compared to a direct calibration. The difference is rather small for  $R$ . For the other assessment indicators the declined model performance is much clearer. Amongst others this can be explained by the rescaling of the donor discharges. Donor catchment selection and rescaling based on the drainage area namely is not a perfect estimating framework for the mean and shape of the discharge signature. Except for the NS coefficient indirect temporal calibration leads to a slightly better model performance than indirect spectral calibration.

## Assessment of indirect calibration

N. De Vleeschouwer and  
V. R. N. Pauwels

Title Page

Abstract

Introduction

Conclusions

References

Tables

Figures

◀

▶

◀

▶

Back

Close

Full Screen / Esc

Printer-friendly Version

Interactive Discussion



Like in experiment 1,  $R$  does not change strongly in the validation period (see Fig. 7, lower-right subplot). BIAS<sub>n</sub> and RMSE<sub>n</sub> on the other hand again increase significantly. Furthermore, a considerable rise of the NS coefficient can be noted for indirect temporal calibration in the validation period. This is not the case for indirect spectral calibration. In case of spatial gauging divergence it seems to be recommended to apply indirect temporal calibration. This should however be nuanced. The spatial dimensions considered in this research are rather small (magnitude kilometers). Due to this proximity the time lapse for a certain meteorological event to happen in the autochtone and donor catchment will be rather small (magnitude minutes-hours). If however the distance between the autochtone and donor catchment is larger the time lapse increases (magnitude hours–days). It is even possible that the same meteorological event will not pass over both catchments. The applicability of indirect temporal calibration should therefore be evaluated in advance based on the proximity between the autochtone and donor catchment.

### 6.2.3 Experiment 3: indirect spectral calibration in case of temporal gauging divergence (setup F-IT-3-0)

In this experiment limited discharge records are available for the autochtone catchments, however, they are not contemporaneous with the forcing records. Specifically for this experiment the time window of the observed discharge time series runs from 1 January 2008 through 31 December 2009. Forcing records are available from 1 January 2006 through 31 December 2007. In this way there is no overlap between the forcing and discharge records. The density spectrum of the observed discharge time series serves as an estimate for the density spectrum of the discharge time series concurrent with the available forcing records. The indicator values of setup F-IT-3-0 in Fig. 7 (lower-left subplot) are based on the discharge simulations over the general calibration period (2006–2009). Both direct spectral calibration and indirect spectral calibration in case of temporal gauging divergence exhibit similar indicator values during the calibration period. Compared to indirect spectral calibration in case of spatial gauging divergence

## Assessment of indirect calibration

N. De Vleeschouwer and  
V. R. N. Pauwels

Title Page

Abstract

Introduction

Conclusions

References

Tables

Figures



Back

Close

Full Screen / Esc

Printer-friendly Version

Interactive Discussion



similar ( $R$ ) or better indicator values (BIAS<sub>n</sub>, RMSE<sub>n</sub> and NS) are obtained in case of temporal gauging divergence. This will be due to the fact that the calibration data are observed at the outlet of the autochtone catchment itself and not in a donor catchment. For the considered dataset interannual discharge variation within the same catchment is thus smaller than discharge variation between the most similar catchments within the same year (in the calibration period). It should be emphasised that in this experiment the non contemporaneous discharge and forcing time series are situated very close together in time. It is not unimaginable that the assessment indicators could turn worse in case of a larger time lapse. For example many former colonies dispose of historical hydrological data because post-colonial civil warfare hindered hydrological monitoring (Winsemius et al., 2006, 2009). These historical time series are often incomplete and are characterised by a larger measurement uncertainty. It is also possible that over time the meteorological conditions or the hydrological response of the catchment change, for example by an atropogene influence (Immerzeel and Droogers, 2008; Coe et al., 2011). All of this can limit the succes of indirect spectral calibration in case of temporal gauging divergence. In the validation period (see Fig. 7, lower-right subplot) the following is observed: all assessment indicators of the indirect spectral calibration (setup F-IT-3-0) are lower than those obtained with direct spectral calibration (setup F-D-3-0). Furthermore all assessment indicators of setup F-IT-3-0 except  $R$  are notably worse compared to those obtained in the calibration period. It can also be concluded that indirect spectral calibration based on limited autochtone discharge time series (setup F-IT-3-0) results in a better model performance than indirect spectral calibration based on rescaled donor discharges (setup F-IS-3-0).

#### 6.2.4 Experiment 4: indirect spectral calibration in case of spatio-temporal gauging divergence (setup F-IST-3-0)

Experiment 4 is a combination of experiment 2 and 3. In this case no discharge observations are available at the outlet of the autochtone catchment. In a very similar donor catchment limited discharge records are available. However, there exist no overlap

## Assessment of indirect calibration

N. De Vleeschouwer and  
V. R. N. Pauwels

Title Page

Abstract

Introduction

Conclusions

References

Tables

Figures

◀

▶

◀

▶

Back

Close

Full Screen / Esc

Printer-friendly Version

Interactive Discussion



between the time windows of the donor discharges and the forcing records in the au-  
tochtone catchment. In this particular experimental design discharge time series are  
available in the donor catchment from 1 January 2008 through 31 December 2009 and  
forcing data from 1 January 2006 through 31 December 2007. The density spectrum  
of the donor discharges will serve as an estimate for the density spectrum of the au-  
tochtone discharge time series concurrent with the available forcing records. Because  
of the double introduced uncertainty in the calibration data it is not illogical to assume  
that calibration setup F-IST-3-0 would lead to a poorer model performance than setups  
F-IT-3-0 and F-IS-3-0. However, the assessment indicators in the calibration and valida-  
tion period (see Fig. 7, lower subplots) show other results. In the calibration period the  
assessment indicators of setup F-IST-3-0 are comparable to those of setup F-IS-3-0.  
Only the NS coefficient is rather lower. The validation period shows different relation-  
ships. The BIAS<sub>n</sub> and RMSE<sub>n</sub> are remarkably better in this combined experiment than  
in the previous two experiments. The *R* and NS coefficient are again comparable to the  
previous indirect spectral calibrations.

As illustration in Figs. 9 and 10 the scatterplots are shown resulting from the di-  
rect temporal calibration setup (T-D) and the four indirect calibration setups (T-IS,  
F-IS-3-0, F-IT-3-0 and F-IST-3-0) for, respectively catchment Oostkamp–Rivierbeek  
and Rummen–Melsterbeek. In the former catchments very good indirect estimates of  
the calibration data are obtained, in the latter catchment those estimates have a lower  
quality.

## 7 Conclusions

In this paper, an assessment is made of indirect calibration of the PDM for six (au-  
tochtone) catchments in Flanders, considered to be ungauged. As calibration algorithm  
PSO is applied. The described results are based on rather small catchments (mag-  
nitude 10–100 km<sup>2</sup>) with a high proximity to each other (magnitude kilometers). The  
different calibration setups are evaluated on the basis of four assessment indicators

## Assessment of indirect calibration

N. De Vleeschouwer and  
V. R. N. Pauwels

Title Page

Abstract

Introduction

Conclusions

References

Tables

Figures



Back

Close

Full Screen / Esc

Printer-friendly Version

Interactive Discussion



( $R$ ,  $BIAS_n$ ,  $RMSE_n$  and  $NS$ ). Those are averaged over the six autochtone catchments. Consequently, the discussed results are valid for an average catchment in Flanders. The first calibration experiment focuses on direct spectral calibration. For this, the root squared spectral densities of the autochtone discharge time series are incorporated in the objective function. The experiment revealed that higher values for the maximum lag of the correlation function ( $\tau_{max}$ ) result in a better model performance during the calibration period. This is not necessarily the case in the validation period. This may be due to an overfitting. Furthermore giving more weight to certain parts of the density spectrum during the spectral calibration generally does not lead to better model performances. In experiments 2, 3 and 4 indirect calibration is examined in, respectively the cases of spatial, temporal and spatio-temporal gauging divergence. In those cases the calibration is, respectively based on the root squared spectral densities of, respectively rescaled donor discharge records, non overlapping autochtone discharge records and non overlapping rescaled donor discharge records. Except for some specific indicator values, the model performance decreased compared to direct calibration but remained at an acceptable level. With regard to indirect calibration in the case of spatial gauging divergence, slightly better results were obtained using indirect temporal calibration vs. indirect spectral calibration. Indirect temporal calibration is however impossible to execute in the case of temporal and spatio-temporal gauging divergence. Therefore only indirect spectral calibration is applied in experiments 3 and 4. Generally better model performances were obtained in experiment 3 compared to experiment 2. This is due to the high uncertainty associated with the estimation of a density spectrum of an autochtone discharge time series based on donor discharges. For certain catchments this can introduce a bias in the model results. It was expected that the model performance in experiment 4 would be worse than in experiment 2 and 3 because a double source of uncertainty is introduced in the calibration data. However, the assessment indicators show that this does not have to be the case.

This paper has shown that a certain potential exists for indirect calibration of a rainfall-runoff model (in particular indirect spectral calibration) in the case of spatial,

## Assessment of indirect calibration

N. De Vleeschouwer and  
V. R. N. Pauwels

Title Page

Abstract

Introduction

Conclusions

References

Tables

Figures



Back

Close

Full Screen / Esc

Printer-friendly Version

Interactive Discussion



temporal and spatio-temporal gauging divergence in ungauged catchments. Future research may focus on a refinement of the calibration framework (e.g. more complex objective functions, better estimation of the spectral densities, etc.). Furthermore it could be challenging but interesting to examine the link between specific catchment properties (e.g. topography, land cover, hydrological signatures, etc.) and the resulting model performance after indirect calibration. For example it may be worthwhile to test whether indirect spectral calibration is more suitable in catchments with a certain discharge signature.

## Appendix A

### Equations of the PDM

In the following section not further specified variables are model parameters and can be found in Table 1.

In the preparatory first step five constants need to be calculated. The calculation of the maximum store capacity of the soil moisture storage  $S_{\max}$  [mm] is based on the minimum ( $c_{\min}$  [mm]) and maximum absorption capacity ( $c_{\max}$  [mm]):

$$S_{\max} = \frac{b(c_{\min} + c_{\max})}{b + 1}. \quad (\text{A1})$$

The constants  $\delta_1$  [-],  $\delta_2$  [-],  $\omega_0$  [-] and  $\omega_1$  [-] are computed using the time constants of the first ( $k_1$  [h]) and second surface storage ( $k_2$  [h]):

$$\delta_1 = e^{-\frac{1}{k_1}} + e^{-\frac{1}{k_2}} \quad (\text{A2})$$

$$\delta_2 = e^{-\frac{1}{k_1}} e^{-\frac{1}{k_2}} \quad (\text{A3})$$

$$\omega_0 = \frac{k_1(e^{-\frac{1}{k_1}} - 1) - k_2(e^{-\frac{1}{k_2}} - 1)}{k_2 - k_1} \quad (\text{A4})$$

## Assessment of indirect calibration

N. De Vleeschouwer and  
V. R. N. Pauwels

Title Page

Abstract

Introduction

Conclusions

References

Tables

Figures

◀

▶

◀

▶

Back

Close

Full Screen / Esc

Printer-friendly Version

Interactive Discussion



$$\omega_1 = \frac{k_2(e^{-\frac{1}{k_2}} - 1)e^{-\frac{1}{k_1}} - k_1(e^{-\frac{1}{k_1}} - 1)e^{-\frac{1}{k_2}}}{k_2 - k_1}. \quad (A5)$$

The actual evapotranspiration aET [mm h<sup>-1</sup>] is calculated on the basis of the potential evapotranspiration pET [mm h<sup>-1</sup>], the store capacity in the soil moisture storage S<sub>1</sub> [mm] at the previous time step and S<sub>max</sub> [mm].

$$aET(t) = pET(t) \left( 1 - \left[ \frac{S_{\max} - S_1(t-1)}{S_{\max}} \right]^{b_e} \right) \quad (A6)$$

For the calculation of the drainage Q<sub>dr</sub> [mm h<sup>-1</sup>], S<sub>1</sub> [mm] of the previous time step and the parameters k<sub>g</sub> [h mm<sup>-2</sup>], S<sub>t</sub> [mm] and b<sub>g</sub> [-] are required:

$$\begin{aligned} \text{if } S_1(t-1) \leq S_t \\ Q_{dr}(t) = 0 \end{aligned}$$

$$\begin{aligned} \text{if } S_1(t-1) > S_t \\ Q_{dr}(t) = \frac{1}{k_g} (S_1(t-1) - S_t)^{b_g}. \end{aligned} \quad (A7)$$

Next, the net precipitation π [mm h<sup>-1</sup>] can be calculated as follows:

$$\pi(t) = P(t) - aET(t) - Q_{dr}(t). \quad (A8)$$

Consequently the direct runoff Q<sub>di</sub> [mm h<sup>-1</sup>] can be computed using the critical store capacity C\* [mm] of the previous time step, π [mm h<sup>-1</sup>] and the parameters c<sub>min</sub> [mm], c<sub>max</sub> [mm] and b [-]:

## Assessment of indirect calibration

N. De Vleeschouwer and  
V. R. N. Pauwels

Title Page

Abstract

Introduction

Conclusions

References

Tables

Figures

◀

▶

◀

▶

Back

Close

Full Screen / Esc

Printer-friendly Version

Interactive Discussion



if  $C^*(t-1) + \pi(t) < c_{\max}$

$$Q_{\text{di}}(t) = \pi(t) - \frac{c_{\max} - c_{\min}}{b+1} \left[ \frac{c_{\max} - C^*(t-1)}{c_{\max} - c_{\min}} \right]^{b+1} + \frac{c_{\max} - c_{\min}}{b+1} \left[ \frac{c_{\max} - C^*(t-1) - \pi(t)}{c_{\max} - c_{\min}} \right]^{b+1} \quad (\text{A9})$$

if  $C^*(t-1) + \pi(t) \geq c_{\max}$

$$Q_{\text{di}}(t) = \pi(t) - \frac{c_{\max} - c_{\min}}{b+1} \left( \left[ \frac{c_{\max} - C^*(t-1)}{c_{\max} - c_{\min}} \right]^{b+1} \right) + C^*(t-1) + \pi(t) - c_{\max}.$$

Once  $\pi$  [ $\text{mm h}^{-1}$ ] and  $Q_{\text{di}}$  [ $\text{mm h}^{-1}$ ] are known for the current time step  $S_1$  [mm] can be calculated for the current time step:

if  $S_1(t) \leq 0$

$$S_1(t) = 0$$

if  $0 < S_1(t) < S_{\max}$

$$S_1(t) = S_1(t-1) + \pi(t) - Q_{\text{di}}(t) \quad (\text{A10})$$

if  $S_1(t) \geq S_{\max}$

$$S_1(t) = S_{\max}.$$

5  $C^*$  [mm] can be calculated on the current time step on the basis of  $S_1$  [mm] at the current time step,  $S_{\max}$  [mm] and the parameters  $c_{\min}$  [mm],  $c_{\max}$  [mm] and  $b$  [-].

## Assessment of indirect calibration

N. De Vleeschouwer and  
V. R. N. Pauwels

Title Page

Abstract

Introduction

Conclusions

References

Tables

Figures

◀

▶

◀

▶

Back

Close

Full Screen / Esc

Printer-friendly Version

Interactive Discussion



$$\begin{aligned} \text{if } C^*(t) &\leq 0 \\ C^*(t) &= 0 \end{aligned}$$

$$\text{if } C^*(t) \geq c_{\max}$$

$$C^*(t) = c_{\max} - (c_{\max} - c_{\min}) \left( \left[ \frac{S_{\max} - S_1(t)}{S_{\max} - c_{\min}} \right]^{\frac{1}{b+1}} \right) \quad (\text{A11})$$

$$\text{if } C^*(t) \geq c_{\max}$$

$$C^*(t) = c_{\max}$$

The capacity store of the subsurface storage  $S_3$  [mm] is computed using  $S_3$  at the previous time step,  $Q_{\text{dr}}$  at the current time step and the parameter  $k_b$  [h].

$$S_3(t) = S_3(t-1) - \frac{e^{-3k_b S_3^2(t-1)} - 1}{3k_b S_3^2(t-1)} (Q_{\text{dr}}(t) - k_b S_3^3(t-1)) \quad (\text{A12})$$

5 Making use of  $S_3$  [mm] and  $k_b$  [h] the base flow  $Q_b$  [mm h<sup>1</sup>] can be calculated:

$$\text{if } Q_b(t) \leq 0$$

$$Q_b(t) = 0$$

$$\text{if } Q_b(t) > 0$$

$$Q_b(t) = k_b S_3^3(t).$$

(A13)

The surface runoff  $Q_r$  [mm h<sup>1</sup>] is calculated as follows:

$$Q_r(t) = -\delta_1 Q_r(t-1) - \delta_2 Q_r(t-2) + \omega_0 Q_d(t) + \omega_1 Q_d(t-1). \quad (\text{A14})$$

10 Eventually the total discharge  $Q_t$  [mm h<sup>1</sup>] can be calculated as the sum of  $Q_r$  en  $Q_b$ : can be calculated on the current time

$$Q_t(t) = Q_r(t) + Q_b(t). \quad (\text{A15})$$

## Assessment of indirect calibration

N. De Vleeschouwer and  
V. R. N. Pauwels

Title Page

Abstract

Introduction

Conclusions

References

Tables

Figures

◀

▶

◀

▶

Back

Close

Full Screen / Esc

Printer-friendly Version

Interactive Discussion



*Acknowledgements.* The time series and spatial data analysed in this research were provided by, respectively the Flemish Environment Agency (VMM) and the Flemish Geographical Information Agency (FGIA). The authors wish to express their appreciation for this data provision. Furthermore a special acknowledgement is owed to Gabriëlle De Lannoy for her advice during the research.

## References

- Beven, K. and Binley, A.: The future of distributed models: model calibration and uncertainty prediction, *Hydrol. Process.*, 6, 279–298, doi:10.1002/hyp.3360060305, 1992. 116
- Brown, R. G. and Hwang, P. Y. C.: *Introduction to Random Signals and Applied Kalman Filtering*, John Wiley & Sons, New York, 1992. 107
- Cabus, P.: River flow prediction through rainfall-runoff modelling with a probability-distributed model (PDM) in Flanders, Belgium, *Agr. Water Manage.*, 95, 859–868, doi:10.1016/j.agwat.2008.02.013, 2008. 108
- Coe, M. T., Latrubesse, E. M., Ferreira, M. E., and Amsler, M. L.: The effects of deforestation and climate variability on the streamflow of the Araguaia River, Brazil, *Biogeochemistry*, 105, 119–131, doi:10.1007/s10533-011-9582-2, 2011. 120
- Duan, Q., Sorooshian, S., and Gupta, V.: Effective and efficient global optimization for conceptual rainfall-runoff models, *Water Resour. Res.*, 28, 1015–1031, doi:10.1029/91WR02985, 1992. 105
- Dunne, T. and Black, R.: Partial area contributions to storm runoff in a small New-England watershed, *Water Resour. Res.*, 6, 1296, doi:10.1029/WR006i005p01296, 1970. 108
- Gan, T. and Biftu, G.: Automatic calibration of conceptual rainfall-runoff models: optimization algorithms, catchment conditions, and model structure, *Water Resour. Res.*, 32, 3513–3524, doi:10.1029/95WR02195, 1996. 105
- Gill, M. K., Kaheil, Y. H., Khalil, A., McKee, M., and Bastidas, L.: Multiobjective particle swarm optimization for parameter estimation in hydrology, *Water Resour. Res.*, 42, W07417, doi:10.1029/2005WR004528, 2006. 115
- Immerzeel, W. W. and Droogers, P.: Calibration of a distributed hydrological model based on satellite evapotranspiration, *J. Hydrol.*, 349, 411–424, doi:10.1016/j.jhydrol.2007.11.017, 2008. 120

## Assessment of indirect calibration

N. De Vleeschouwer and  
V. R. N. Pauwels

Title Page

Abstract

Introduction

Conclusions

References

Tables

Figures

◀

▶

◀

▶

Back

Close

Full Screen / Esc

Printer-friendly Version

Interactive Discussion



- Jenson, S. and Domingue, J.: Extracting topographic structure from digital elevation data for geographic information-system analysis, *Photogramm. Eng. Rem. S.*, 54, 1593–1600, 1988. 108
- Kennedy, J. and Eberhart, R.: Particle swarm optimization, in: *Neural Networks, 1995, Proceedings, IEEE International Conference on*, vol. 4, 1942–1948, doi:10.1109/ICNN.1995.488968, 1995. 105, 115
- Liu, J. and Han, D.: Indices for calibration data selection of the rainfall-runoff model, *Water Resour. Res.*, 46, W04512, doi:10.1029/2009WR008668, 2010. 115
- Montanari, A. and Toth, E.: Calibration of hydrological models in the spectral domain: An opportunity for scarcely gauged basins?, *Water Resour. Res.*, 43, W05434, doi:10.1029/2006WR005184, 2007. 106
- Moore, R. J.: The PDM rainfall-runoff model, *Hydrol. Earth Syst. Sci.*, 11, 483–499, doi:10.5194/hess-11-483-2007, 2007. 106, 135
- Mousavi, S. J. and Shourian, M.: Adaptive sequentially space-filling metamodeling applied in optimal water quantity allocation at basin scale, *Water Resour. Res.*, 46, W03520, doi:10.1029/2008WR007076, 2010. 115
- Papoulis, A.: *Probability, Random Variables and Stochastic Processes*, McGraw Hill, New York, 1965. 107
- Pauwels, V. R. N. and De Lannoy, G. J. M.: Multivariate calibration of a water and energy balance model in the spectral domain, *Water Resour. Res.*, 47, W07523, doi:10.1029/2010WR010292, 2011. 106, 115, 116
- Quets, J. J., De Lannoy, G. J. M., and Pauwels, V. R. N.: Comparison of spectral and time domain calibration methods for precipitation-discharge processes, *Hydrol. Process.*, 24, 1048–1062, doi:10.1002/hyp.7546, 2010. 106, 116
- Reed, P., Minsker, B., and Goldberg, D.: Designing a competent simple genetic algorithm for search and optimization, *Water Resour. Res.*, 36, 3757–3761, doi:10.1029/2000WR900231, 2000. 105
- Scheerlinck, K., Pauwels, V. R. N., Vernieuwe, H., and De Baets, B.: Calibration of a water and energy balance model: Recursive parameter estimation versus particle swarm optimization, *Water Resour. Res.*, 45, W10422, doi:10.1029/2009WR008051, 2009. 105, 115
- Shannon, C.: Communication in the presence of noise (reprinted), *Proc. IEEE*, 72, 1192–1201, doi:10.1109/PROC.1984.12998, 1984. 107

## Assessment of indirect calibration

N. De Vleeschouwer and  
V. R. N. Pauwels

Title Page

Abstract

Introduction

Conclusions

References

Tables

Figures

◀

▶

◀

▶

Back

Close

Full Screen / Esc

Printer-friendly Version

Interactive Discussion



- Sivapalan, M., Takeuchi, K., Franks, S., Gupta, V., Karambiri, H., Lakshmi, V., Liang, X., McDonnell, J., Mendiondo, E., O'Connell, P., Oki, T., Pomeroy, J., Schertzer, D., Uhlenbrook, S., and Zehe, E.: IAHS decade on Predictions in Ungauged Basins (PUB), 2003–2012: shaping an exciting future for the hydrological sciences, *Hydrolog. Sci. J.*, 48, 857–880, doi:10.1623/hysj.48.6.857.51421, 2003. 105
- Thyer, M., Kuczera, G., and Bates, B.: Probabilistic optimization for conceptual rainfall-runoff models: A comparison of the shuffled complex evolution and simulated annealing algorithms, *Water Resour. Res.*, 35, 767–773, doi:10.1029/1998WR900058, 1999. 105
- Tolson, B. A., Asadzadeh, M., Maier, H. R., and Zecchin, A.: Hybrid discrete dynamically dimensioned search (HD-DDS) algorithm for water distribution system design optimization, *Water Resour. Res.*, 45, W12416, doi:10.1029/2008WR007673, 2009. 115
- Whittle, P.: Estimation and information in stationary time series, *Ark. Mat.*, 2, 423–434, doi:10.1007/BF02590998, 1953. 106
- Winsemius, H. C., Savenije, H. H. G., Gerrits, A. M. J., Zapreeva, E. A., and Klees, R.: Comparison of two model approaches in the Zambezi river basin with regard to model reliability and identifiability, *Hydrol. Earth Syst. Sci.*, 10, 339–352, doi:10.5194/hess-10-339-2006, 2006. 120
- Winsemius, H. C., Schaefli, B., Montanari, A., and Savenije, H. H. G.: On the calibration of hydrological models in ungauged basins: A framework for integrating hard and soft hydrological information, *Water Resour. Res.*, 45, W12422, doi:10.1029/2009WR007706, 2009. 106, 120
- Zhang, Y. and Chiew, F. H. S.: Relative merits of different methods for runoff predictions in ungauged catchments, *Water Resour. Res.*, 45, W07412, doi:10.1029/2008WR007504, 2009. 115

**Assessment of indirect calibration**N. De Vleeschouwer and  
V. R. N. Pauwels

Title Page

Abstract

Introduction

Conclusions

References

Tables

Figures

◀

▶

◀

▶

Back

Close

Full Screen / Esc

Printer-friendly Version

Interactive Discussion



## Assessment of indirect calibration

N. De Vleeschouwer and  
V. R. N. Pauwels

**Table 1.** Overview of the PDM parameters with indication of the lower and upper boundaries for catchments in Flanders.

Parameter	Units	Lower boundary	Upper boundary
$c_{\max}$	[mm]	160	5000
$c_{\min}$	[mm]	0	300
$b$	[-]	0.1	2
$b_e$	[-]	1	2
$k_1$	[h]	0.9	40
$k_2$	[h]	0.1	15
$k_b$	[h]	0	5000
$k_g$	[hmm <sup>-2</sup> ]	700	25 000
$S_t$	[mm]	0	150
$b_g$	[-]	1	1
tdly	[h]	0	10
$q_c$	[m <sup>3</sup> s <sup>-1</sup> ]	-4.08	0.03

[Title Page](#)
[Abstract](#)
[Introduction](#)
[Conclusions](#)
[References](#)
[Tables](#)
[Figures](#)
[◀](#)
[▶](#)
[◀](#)
[▶](#)
[Back](#)
[Close](#)
[Full Screen / Esc](#)
[Printer-friendly Version](#)
[Interactive Discussion](#)






## Assessment of indirect calibration

N. De Vleeschouwer and  
V. R. N. Pauwels

**Table 4.** Overview of the applied calibration setups.

Experiment	Code	Domain	Gauging divergence	$\tau_{\max}$ [months]	Weight type
1, 2, 3, 4	T-D	Time	/	/	/
1	F-D-1-0	Frequency	/	1	/
1, 2	F-D-3-0	Frequency	/	2	/
1	F-D-12-0	Frequency	/	3	/
1	F-D-3-1	Frequency	/	3	1
1	F-D-3-2	Frequency	/	3	2
1	F-D-3-3	Frequency	/	3	3
2	T-IS	Time	Spatial	/	/
2	F-IS-3-0	Frequency	Spatial	3	/
3	F-IT-3-0	Frequency	Temporal	3	/
4	F-IST-3-0	Frequency	Spatio temporal	3	/

[Title Page](#)
[Abstract](#)
[Introduction](#)
[Conclusions](#)
[References](#)
[Tables](#)
[Figures](#)
[Back](#)
[Close](#)
[Full Screen / Esc](#)
[Printer-friendly Version](#)
[Interactive Discussion](#)


# HESSD

10, 103–144, 2013

## Assessment of indirect calibration

N. De Vleeschouwer and  
V. R. N. Pauwels[Title Page](#)[Abstract](#)[Introduction](#)[Conclusions](#)[References](#)[Tables](#)[Figures](#)[⏪](#)[⏩](#)[◀](#)[▶](#)[Back](#)[Close](#)[Full Screen / Esc](#)[Printer-friendly Version](#)[Interactive Discussion](#)

**Table 5.** Overview of PSO algorithm parameters.

Parameter	Description
$N_j$	Particle population size
$N_k$	Iterations
$c_1$	Cognitive parameter
$c_2$	Social parameter
$w$	Inertia weight
$\delta$	Velocity limiter

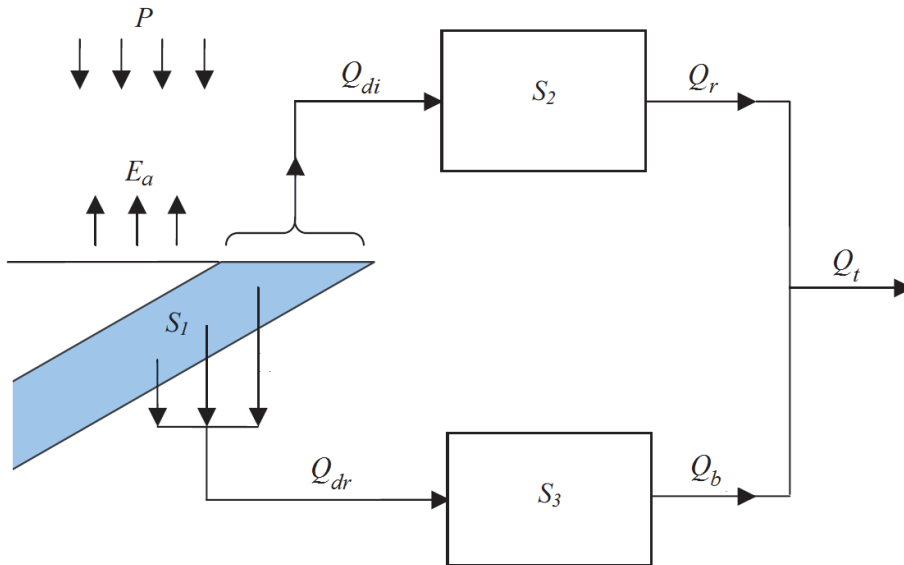


**Fig. 1.** General model structure of the PDM (Moore, 2007).

## Assessment of indirect calibration

N. De Vleeschouwer and  
V. R. N. Pauwels

Title Page

Abstract

Introduction

Conclusions

References

Tables

Figures

◀

▶

◀

▶

Back

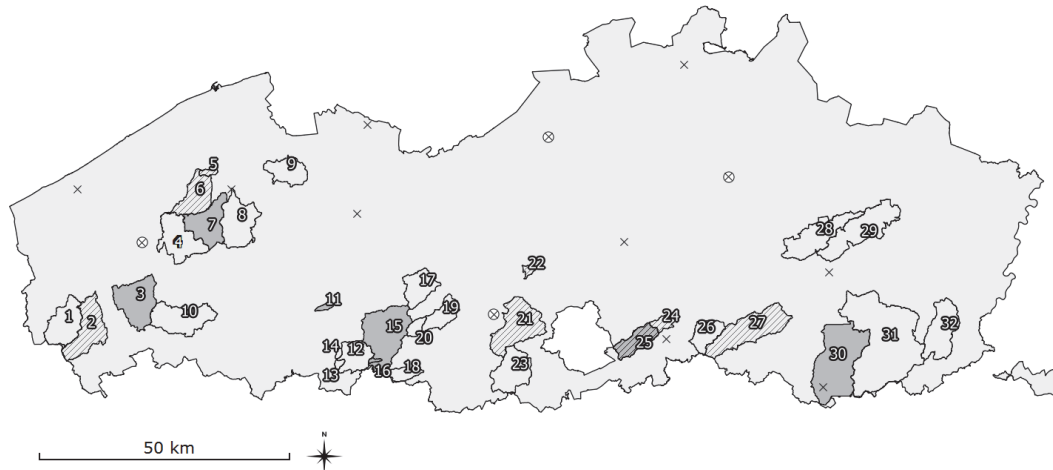
Close

Full Screen / Esc

Printer-friendly Version

Interactive Discussion



**Assessment of  
indirect calibration**N. De Vleeschouwer and  
V. R. N. Pauwels

**Fig. 2.** The spatial spreading of the 32 catchments included in this study. The autochtone catchments considered to be ungauged are colored gray, the donor catchments are filled in with a diagonal line pattern. Stations with precipitation and potential evapotranspiration measurement are indicated with, respectively crosses and circles.

Title Page

Abstract

Introduction

Conclusions

References

Tables

Figures

◀

▶

◀

▶

Back

Close

Full Screen / Esc

Printer-friendly Version

Interactive Discussion



## Assessment of indirect calibration

N. De Vleeschouwer and  
V. R. N. Pauwels

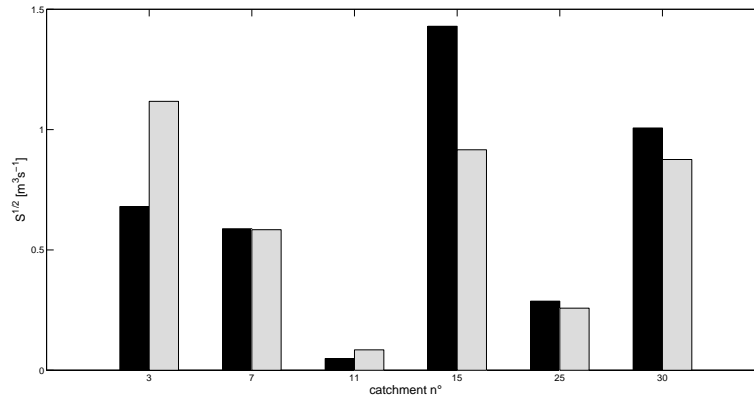


**Fig. 3.** Actual (black) vs. estimated (gray) root squared spectral density ( $k = 0$ ) of the discharge time series for the six autochtone catchments in case of spatial gauging divergence (period 2006–2009). The estimates are rescaled root squared densities of the donor discharge time series.

[Title Page](#)
[Abstract](#)
[Introduction](#)
[Conclusions](#)
[References](#)
[Tables](#)
[Figures](#)
[⏪](#)
[⏩](#)
[◀](#)
[▶](#)
[Back](#)
[Close](#)
[Full Screen / Esc](#)
[Printer-friendly Version](#)
[Interactive Discussion](#)


## Assessment of indirect calibration

N. De Vleeschouwer and  
V. R. N. Pauwels

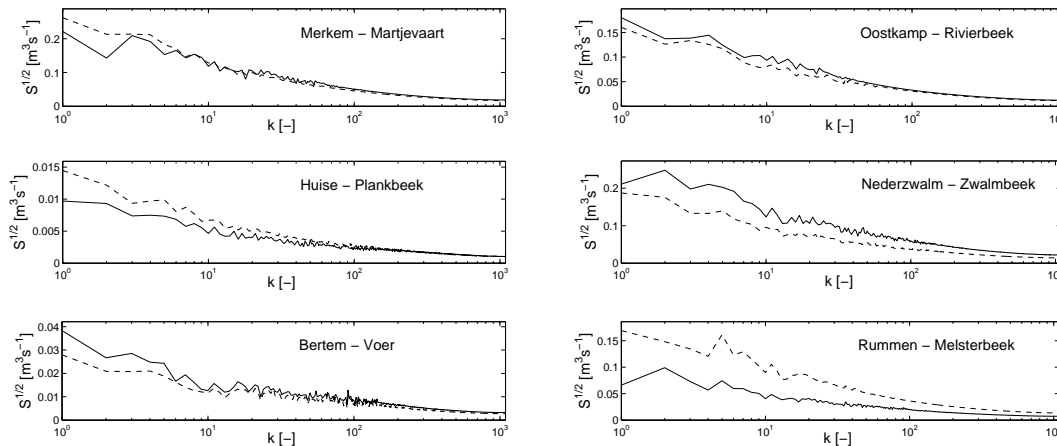


**Fig. 4.** Actual (solid line) vs. estimated (dashed line) root squared density spectrum ( $k > 0$ ) of the discharge time series for the six autochthonous catchments in case of spatial gauging divergence (period 2006–2009). The estimates are rescaled root squared densities of the donor discharge time series.

[Title Page](#)
[Abstract](#)
[Introduction](#)
[Conclusions](#)
[References](#)
[Tables](#)
[Figures](#)
[◀](#)
[▶](#)
[◀](#)
[▶](#)
[Back](#)
[Close](#)
[Full Screen / Esc](#)
[Printer-friendly Version](#)
[Interactive Discussion](#)


## Assessment of indirect calibration

N. De Vleeschouwer and  
V. R. N. Pauwels

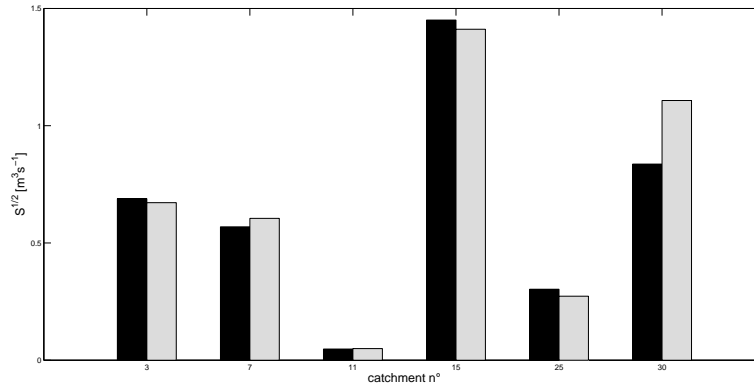


**Fig. 5.** Actual (black) vs. estimated (gray) root squared spectral density ( $k = 0$ ) of the discharge time series for the six autochthonous catchments in case of temporal gauging divergence (period 2006–2007). The estimates are root squared densities of the autochthonous discharge time series during the period 2008–2009.

[Title Page](#)
[Abstract](#)
[Introduction](#)
[Conclusions](#)
[References](#)
[Tables](#)
[Figures](#)
[◀](#)
[▶](#)
[◀](#)
[▶](#)
[Back](#)
[Close](#)
[Full Screen / Esc](#)
[Printer-friendly Version](#)
[Interactive Discussion](#)




## Assessment of indirect calibration

N. De Vleeschouwer and  
V. R. N. Pauwels

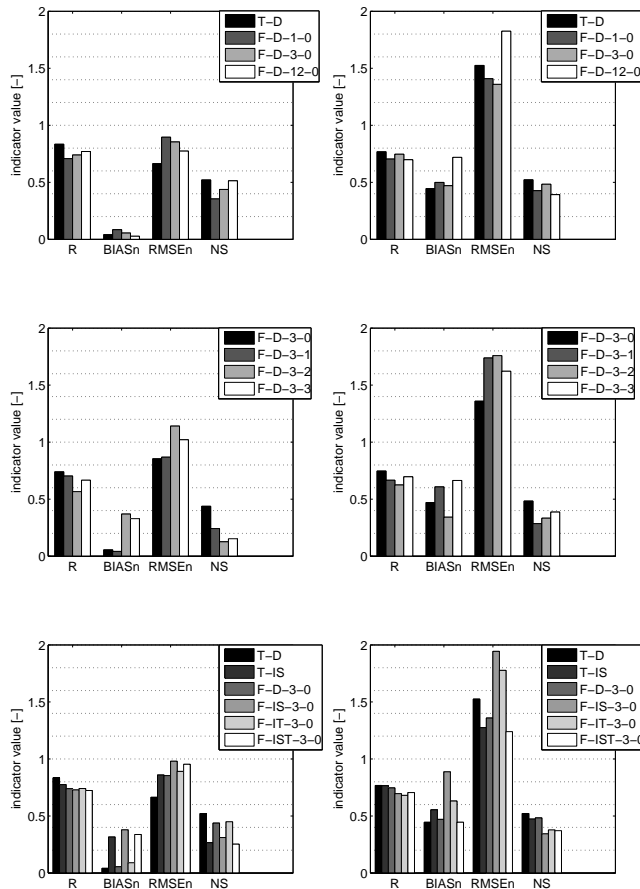


**Fig. 7.** Comparative bar charts of the assessment indicator values for the different calibration setups. Left panels: calibration period, right panels: validation period.

Title Page

Abstract Introduction

Conclusions References

Tables Figures

◀ ▶

◀ ▶

Back Close

Full Screen / Esc

Printer-friendly Version

Interactive Discussion



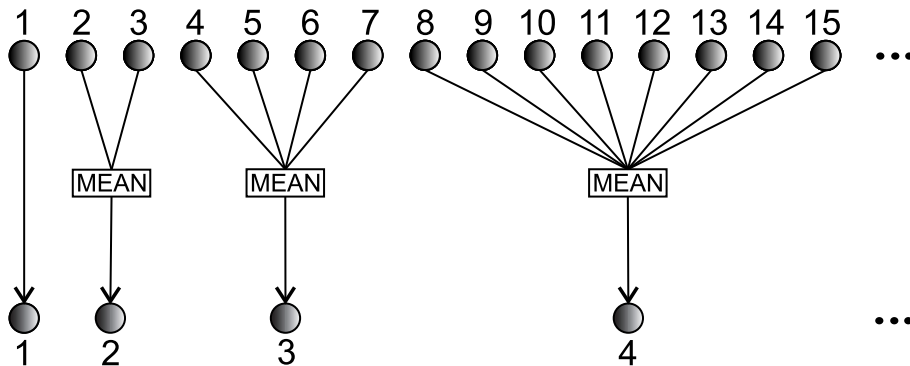


Fig. 8. Principle of exponential clustering and averaging (exponent 2).

## Assessment of indirect calibration

N. De Vleeschouwer and  
V. R. N. Pauwels

Title Page

Abstract

Introduction

Conclusions

References

Tables

Figures

◀

▶

◀

▶

Back

Close

Full Screen / Esc

Printer-friendly Version

Interactive Discussion



## Assessment of indirect calibration

N. De Vleeschouwer and V. R. N. Pauwels

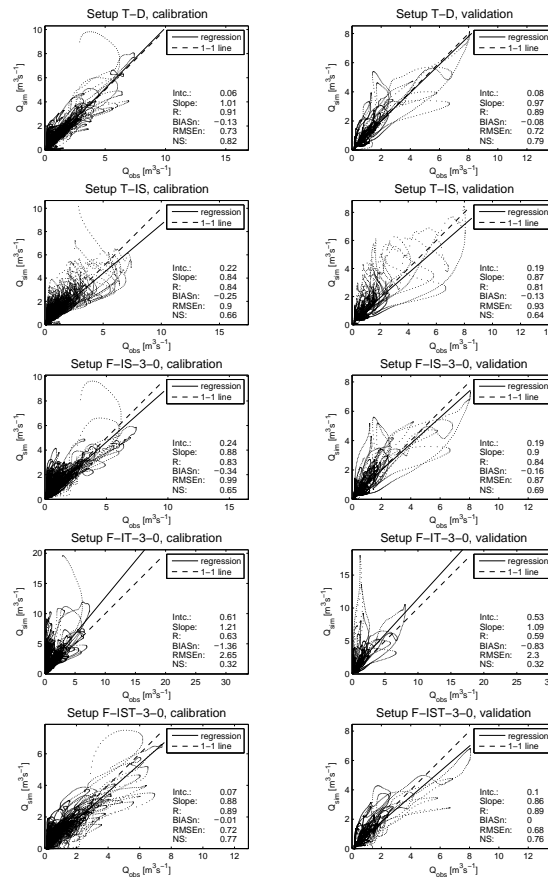


**Fig. 9.** Scatter plots of observed and simulated discharge in catchment Oostkamp–Rivierbeek for calibration setups T-D (1), T-IS (2), F-IS-3-0 (3), F-IT-3-0 (4) and F-IST-3-0 (5) in the calibration (left) and validation (right) period.

Title Page

Abstract

Introduction

Conclusions

References

Tables

Figures

◀

▶

◀

▶

Back

Close

Full Screen / Esc

Printer-friendly Version

Interactive Discussion



## Assessment of indirect calibration

N. De Vleeschouwer and  
V. R. N. Pauwels

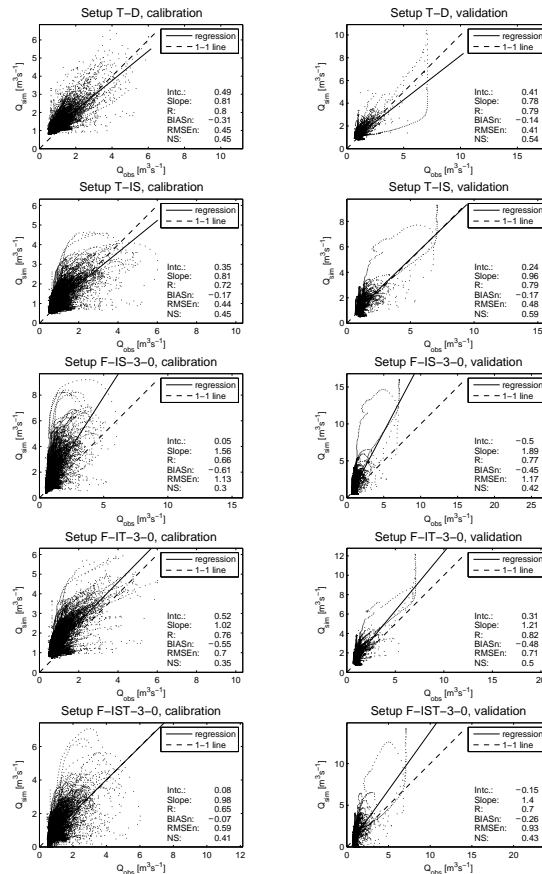


**Fig. 10.** Scatterplots of observed and simulated discharge in catchment Rummen–Melsterbeek for calibration setups T-D (1), T-IS (2), F-IS-3-0 (3), F-IT-3-0 (4) and F-IST-3-0 (5) in the calibration (left) and validation (right) period.

[Title Page](#)
[Abstract](#)
[Introduction](#)
[Conclusions](#)
[References](#)
[Tables](#)
[Figures](#)
[Back](#)
[Close](#)
[Full Screen / Esc](#)
[Printer-friendly Version](#)
[Interactive Discussion](#)